

## Imaging Polyatomic Molecules in Three Dimensions Using Molecular Frame Photoelectron Angular Distributions

J. B. Williams,<sup>1</sup> C. S. Trevisan,<sup>2</sup> M. S. Schöffler,<sup>3</sup> T. Jahnke,<sup>3</sup> I. Bocharova,<sup>4</sup> H. Kim,<sup>3</sup> B. Ulrich,<sup>3</sup> R. Wallauer,<sup>3</sup> F. Sturm,<sup>4</sup> T. N. Rescigno,<sup>4</sup> A. Belkacem,<sup>4</sup> R. Dörner,<sup>3</sup> Th. Weber,<sup>4</sup> C. W. McCurdy,<sup>4,5</sup> and A. L. Landers<sup>1</sup>

<sup>1</sup>*Department of Physics, Auburn University, Auburn, Alabama 36849, USA*

<sup>2</sup>*Department of Sciences and Mathematics, California Maritime Academy, Vallejo, California 94590, USA*

<sup>3</sup>*Institut für Kernphysik, J. W. Goethe Universität, Max-von-Laue-Strasse 1, 60438 Frankfurt, Germany*

<sup>4</sup>*Lawrence Berkeley National Laboratory, Chemical Sciences, Berkeley, California 94720, USA*

<sup>5</sup>*Department of Chemistry, University of California, Davis, California 95616, USA*

(Received 19 January 2012; published 8 June 2012)

We demonstrate a method for determining the full three-dimensional molecular-frame photoelectron angular distribution in polyatomic molecules using methane as a prototype. Simultaneous double Auger decay and subsequent dissociation allow measurement of the initial momentum vectors of the ionic fragments and the photoelectron in coincidence, allowing full orientation by observing a three-ion decay pathway, ( $H^+$ ,  $H^+$ ,  $CH_2^+$ ). We find the striking result that at low photoelectron energies the molecule is effectively imaged by the focusing of photoelectrons along bond directions.

DOI: [10.1103/PhysRevLett.108.233002](https://doi.org/10.1103/PhysRevLett.108.233002)

PACS numbers: 33.80.Eh, 33.60.+q

Imaging molecular structure is a critical challenge in chemical physics recently highlighted by the emergence of techniques that, similar to ultrafast electron diffraction [1] or x-ray diffraction [2], have the potential to be taken to the time domain and thereby ultimately be used to make “movies” of chemical reactions on their natural time scale. Of particular interest is the development of such techniques that can be applied to the dynamics of isolated molecules. Here, the full three-dimensional orientation of a polyatomic molecule is measured simultaneously with the three components of the momentum of a photoelectron ejected from it with no underlying assumptions of symmetry or geometry. We present three-dimensional images of a polyatomic molecule measured with this technique, demonstrating an effect predicted [3] for polyatomic molecules with a heavy central atom bonded to hydrogens, namely that low-energy photoelectrons can directly image the molecular potential and bond structure.

When a photoelectron is launched by photoabsorption of an inner shell, the outgoing photoelectron wave is then scattered by the aggregate potential of the molecule. The final angular distribution in the body-fixed frame of the molecule is an exquisitely sensitive probe of molecular structure and initial electronic state, which has been recently argued and demonstrated [4,5]. However, observing molecular-frame photoelectron angular distributions (MFPADs) at high resolution requires accurate orientation of the molecule in the gas phase. Three-dimensional laser alignment [6,7] can accomplish such orientation prior to photoionization but is limited to molecules with an asymmetric polarizability. In the case of simple diatomic molecules, orientation can also be accomplished by detecting the photoelectron in coincidence with positively charged fragments that emerge following prompt Auger decay and

dissociation [8]. Progress has also been made toward three-dimensional MFPAD measurement using coincidence detection and velocity map imaging [9]. Here we present photoelectron imaging of methane molecules, where *both* the photoelectron momentum and corresponding body frame of the polyatomic molecule are fully determined in all three dimensions.

For many molecules, including  $CH_4$ , core ionization opens a strong simultaneous double Auger decay channel that produces a trication that then can dissociate promptly to three positively charged fragments. Momentum imaging of those three fragments with the photoelectron in coincidence provides a direct and unambiguous measurement of the MFPAD for a polyatomic molecule through the simultaneous orientation of three axes for every ionization event detected. We demonstrate this concept here using *K*-shell photoionization [10] of the methane molecule as a prototype. We find the surprising result that, for photoelectron energies below about 10 eV, the photoelectron tends to be focused along the bond directions, and that, when the MFPAD is averaged over all polarization directions, the result can effectively image the geometry of the molecule.

In order for coincidence measurements to reveal the orientation of a molecule following an ionization event, its dissociation must be prompt and essentially along the directions of the bonds that are ruptured by the loss of valence electrons. In the case of core or inner-shell photoionization followed by a single Auger decay, two valence electrons are lost in the final state and this condition, called “axial recoil” for diatomics, may or may not be satisfied [11]. However, because simultaneous double Auger decay is a strongly populated decay channel in methane, a substantial fraction of photoionization events produce a  $CH_4^{4++}$  trication from which three bonding electrons are

missing. This highly unstable arrangement causes prompt dissociation dynamics where molecule fragments are directed along the ruptured bonds, as can be clearly seen in Fig. 1. The momentum vectors of the three fragments, measured in coincidence, peak very nearly along the bond angles for the  $H^+$  fragments and bisect the bond angle for  $CH_2^+$ . In this case, sequential Auger decay would proceed through the excited dication state with configuration  $1a_g^2 1t_2^6$ , but Hartree-Fock calculations suggest that this pathway is energetically forbidden. Calculations at that level suggest a similar situation in  $NH_3$  but not in water, where nonetheless simultaneous double Auger decay has apparently been observed [9]. Even in cases where simultaneous double Auger decay competes with Auger cascade, it may still be detectable in a coincidence measurement by selecting on ion momenta corresponding to direct breakup, such as those shown in Fig. 1. Thus, the class for which complete 3D MFPADs are measurable with these techniques is likely to include many small molecules.

We used synchrotron radiation produced by the Advanced Light Source's beam line 11.0.2 to photoionize the carbon 1 s electron in methane. The experiment used cold-target recoil-ion momentum spectroscopy (COLTRIMS) [8,12], where a supersonic gas jet of methane intersected a beam of linearly polarized 295 eV photons. The majority of these photoionized molecules relax through single or simultaneous double Auger decay. The resulting di- and trications then dissociate into several fragments. All ions and photoelectrons are guided to position and time-sensitive multihit detectors with weak electric and magnetic fields [13]. The final positions and flight times in fourfold (or fivefold) coincidence for each event are then used to determine the full vector momentum of each particle. The data were taken in event mode, and analyzed off-line.

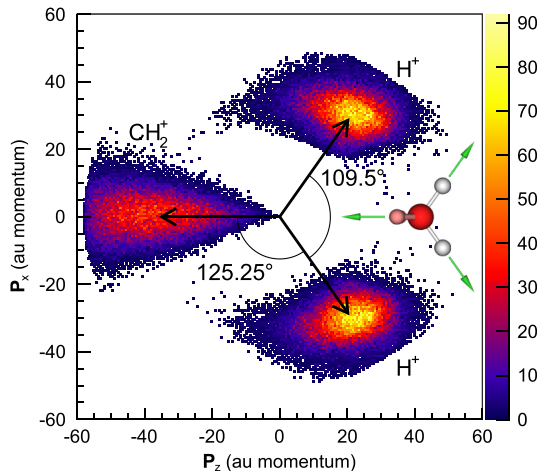


FIG. 1 (color online). Fragment ion momenta in the ( $H^+$ ,  $H^+$ ,  $CH_2^+$ ) dissociation channel following simultaneous double Auger decay of core ionized  $CH_4^+$ . The angles given are those of the equilibrium geometry of methane, as indicated by the inset.

We can verify that the ( $H^+$ ,  $H^+$ ,  $CH_2^+$ ) channel is the result of simultaneous double Auger decay by measuring the momentum distributions of the ejected electrons in coincidence with the ions. In Fig. 2, the bright rings correspond to photoelectrons of  $4.2 \pm 0.2$  eV, and in the channel ( $H^+$ ,  $H^+$ ,  $CH_2$ ) we see discrete lines corresponding to Auger decay into different electronic channels, while in the channel corresponding to the breakup of the trication ( $H^+$ ,  $H^+$ ,  $CH_2^+$ ), we see the energy sharing between two simultaneously ejected electrons. In that case, the energy-sharing distribution is smooth but highly asymmetric [14] and peaks with one electron having nearly zero momentum (the bright dot at the center of the ring) and the other carrying most of the available energy, corresponding to the decay to a particular electronic state of the trication  $p_x \approx 2.6$  and 4 a.u.

The calculation of MFPADs requires a description of both the initial neutral electronic state of the molecule and the electron-ion scattering wave function for an electron scattering from the core-hole cationic state of the molecule. We use the complex Kohn variational method outlined in Refs. [15,16] to calculate the MFPAD defined by the dipole matrix element in the equation,

$$\frac{d^2\sigma^{\Gamma_0}}{d\Omega_{\vec{k}}d\Omega_{\hat{\epsilon}}} = \frac{8\pi\omega}{3c} |\hat{\epsilon} \cdot \langle \Psi_{\Gamma_0, \vec{k}_{\Gamma_0}}^- | \hat{\mu} | \Psi_0 \rangle|^2, \quad (1)$$

which defines the cross section for polarization  $\hat{\epsilon}$  and ejected electron momentum  $\vec{k}_{\Gamma_0}$ , leaving the ion in state  $\Gamma_0$ . The target wave function for the electron-ion calculation is constructed as a single configuration using the natural orbitals from the averaged density matrices of the

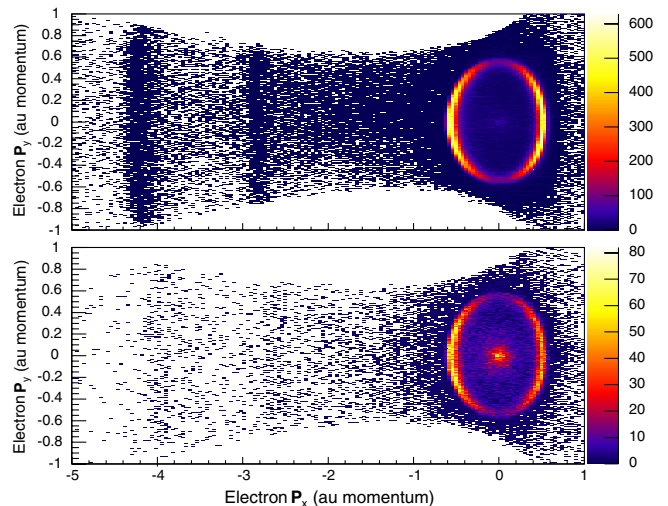


FIG. 2 (color online). Two-dimensional electron momentum distributions with polarization along the  $x$  axis. Top: Measured in coincidence with the ( $H^+$ ,  $H^+$ ,  $CH_2$ ) channel. Bottom: Measured in coincidence with the ( $H^+$ ,  $H^+$ ,  $CH_2^+$ ) channel. Low-energy electron signature at  $p_x = 0$  from simultaneous double Auger decay is visible in the lower panel, while the upper panel shows discrete lines from single Auger decay at  $p_x \approx -4$ .

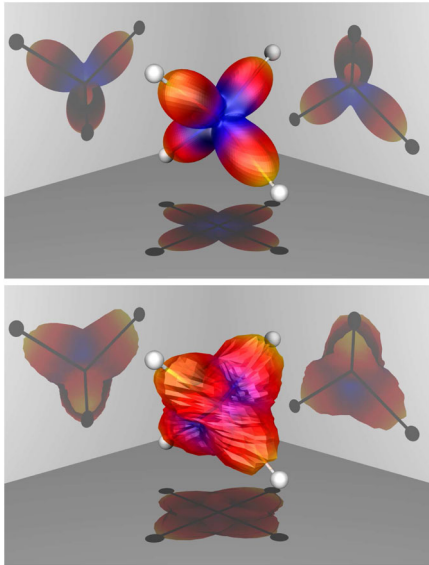


FIG. 3 (color online). Methane imaged via the MFPAD for  $K$ -shell photoelectron. Equilibrium geometry shown to indicate molecular frame. Top: Calculated MFPAD at 4.35 eV integrated over all polarization directions. Bottom: The experimental MFPAD obtained from the  $(\text{H}^+, \text{H}^+, \text{CH}_2^+)$  decay pathway.

ion and neutral molecules, effectively applying Slater's transition state approximation [17] for the photoionization process. The neutral initial state wave function,  $\Psi_0$ , is constructed as a single configuration from those natural orbitals. The complex Kohn scattering calculation then

constructs the final state  $\Psi_{\Gamma_0, \vec{k}\Gamma_0}^-$  by using the static-exchange approximation with the target cation wave function constructed as a single configuration of the same natural orbitals.

At photoelectron kinetic energies below about 10 eV, however, we find more than just the symmetry of the molecule in both the experimental and theoretical MFPADs for methane shown in Fig. 3, where the MFPAD is integrated over all polarization directions thereby isolating the influence of the molecular potential on the photoelectron distribution. We find an image of the geometry of the molecule, revealed by the apparent directing of the outgoing electrons toward the protons for which a simple model has yet to be found. This surprising result is also suggested by Kohn variational calculations of the MFPADs for core ionization of ammonia and water (not shown) [3], and we speculate that, for sufficiently low kinetic energies, core ionization MFPADs may provide a general way to monitor the geometry of small molecules at the time of photoejection. Figure 3 shows the results of measurement of the MFPAD in the trication channel,  $(\text{H}^+, \text{H}^+, \text{CH}_2^+)$ , which is the general procedure we propose for 3D MFPAD measurements when simultaneous double Auger decay can be detected. The remaining small discrepancy between theory and experiment we attribute primarily to a combination of (1) the broad gating and binning of the statistics-limited experimental data, (2) the angular resolution of the measurement, and (3) the zero-point vibrational motion of the molecule.

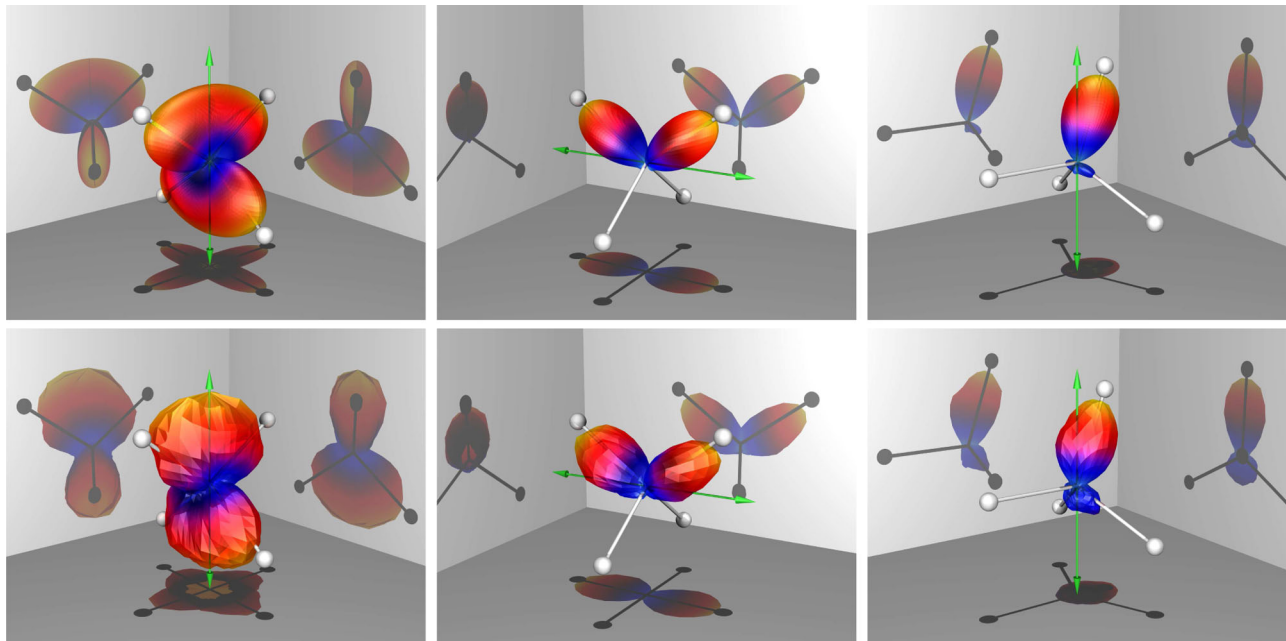


FIG. 4 (color online). Theoretical (top) and experimental (bottom) MFPADs for particular orientations of the polarization axis in the molecular frame. Left column: Polarization axis aligned to a  $C_2$  symmetry axis. Middle column: Polarization axis perpendicular to a  $C_2$  axis and in the plane of two hydrogen bonds. Right column: Polarization axis perpendicular to a  $C_3$  axis along one bond and in plane with another bond.

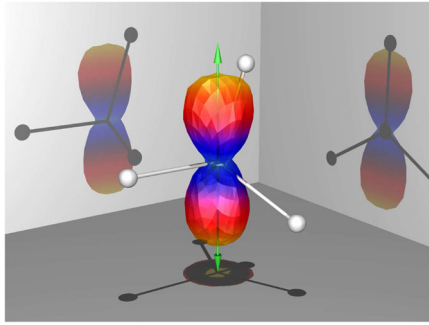


FIG. 5 (color online). MFPAD for the case of large photoelectron energy ( $\approx 16$  eV) following simultaneous double Auger decay of core ionized  $\text{CH}_4^+$ . Here, the molecular potential has little influence on the dipole distribution of the photoelectron.

Low-energy (4.35 eV) MFPADs with the polarization at various angles relative to the molecule shown in Fig. 4 demonstrate a competition between two effects that primarily determine the shapes of the MFPADs. The first is the evident propensity of the outgoing electrons to be ejected in the directions of the bonds by scattering from the molecular potential. The second is the initial  $1s \rightarrow \epsilon p$  transition that sends the electron out along the axis of polarization. More specifically, the cross sections are each coherent combinations of the  $x$ ,  $y$ ,  $z$  components of the dipole transition amplitude in Eq. (1) and, as such, are expected to be even more sensitive to the molecular geometry than the incoherent sum that determines the MFPAD in Fig. 3. Nonetheless, the agreement between theory and experiment is nearly exact, and this fact suggests that it may be generally sufficient to apply the relatively simple approximation used here, in which the scattering wave function for the ejected core electron can be computed by a single-channel, static-exchange treatment. Calculations at the level of theory presented here suggest that this imaging effect should be visible in methane, water, and ammonia at energies less than about 10 eV. The measurements and calculations reported here 4.35 eV (0.16 hartree) are roughly in the middle of that range for methane [3].

We see additional evidence for the energy-dependent influence of the molecular potential in Fig. 5, which shows the MFPAD for 16 eV photoelectron energy for a molecule oriented relative to the polarization axis. The distribution is essentially dipole in nature, indicating that the molecular potential has little apparent influence over the photoelectron emission for this case.

The results presented here suggest that 3D MFPADs from core ionization can be used as a probe of molecular geometry in ultrafast time-dependent measurements of molecular dynamics, whether the molecule is laser aligned or oriented by coincidence measurements following simultaneous double Auger decay. The dissociation dynamics following simultaneous double Auger decay, leading to a trication with three missing valence electrons, can be expected to be more frequently

direct and prompt than the case of single Auger decay, and therefore they provide a general tool for 3D molecular orientation.

In the short term, this technique may allow direct exploration of questions such as core-localization dynamics in the carbon atoms of ethane or other symmetric hydrocarbons, and whether the lone pairs in ammonia and water might have a simple influence on core photoelectron emission at low energies. Since photon pulses from higher harmonic sources and free-electron lasers are already providing, or will soon provide, pulses in the attosecond domain, this imaging technique will likely prove to be a valuable tool for observing molecular conformation changes in real time in molecules that have been laser aligned.

This work was supported in part by the U.S. Department of Energy Office of Basic Energy Sciences, Division of Chemical Sciences Contracts No. DE-AC02-05CH11231 and No. DE-FG02-10ER16146. C. S. T. acknowledges support from a CSU Maritime SoTL grant. Additional funding was provided by Deutsche Forschungsgemeinschaft and DAAD.

- 
- [1] A. H. Zewail, *Science* **328**, 187 (2010).
  - [2] H. N. Chapman *et al.*, *Nature (London)* **470**, 73 (2011).
  - [3] C. S. Trevisan, C. W. McCurdy, and T. N. Rescigno (unpublished).
  - [4] Y. Arasaki, K. Takatsuka, K. Wang, and V. McKoy, *J. Chem. Phys.* **132**, 124307 (2010).
  - [5] P. Hockett, C. Z. Bisgaard, O. J. Clarkin, and A. Stolow, *Nature Phys.* **7**, 612 (2011).
  - [6] J. J. Larsen, K. Hald, N. Bjerre, H. Stapelfeldt, and T. Seideman, *Phys. Rev. Lett.* **85**, 2470 (2000).
  - [7] J. L. Hansen *et al.*, *Phys. Rev. A* **83**, 023406 (2011).
  - [8] A. Landers *et al.*, *Phys. Rev. Lett.* **87**, 013002 (2001).
  - [9] M. Yamazaki, J. Adachi, T. Teramoto, A. Yagishita, M. Stener, and P. Decleva, *J. Phys. B* **42**, 051001 (2009).
  - [10] R. Flammini, M. Satta, E. Fainelli, G. Alberti, F. Maracci, and L. Avaldi, *New J. Phys.* **11**, 083006 (2009).
  - [11] T. Weber *et al.*, *J. Phys. B* **34**, 3669 (2001).
  - [12] R. Dörner, V. Mergel, O. Jagutzki, L. Spielberger, J. Ullrich, R. Moshhammer, and H. Schmidt-Böcking, *Phys. Rep.* **330**, 95 (2000).
  - [13] O. Jagutzki, J. S. Lapington, L. B. C. Worth, U. Spillman, V. Mergel, and H. Schmidt-Böcking, *Nucl. Instrum. Methods Phys. Res., Sect. A* **477**, 256 (2002).
  - [14] J. Viefhaus, A. N. Grum-Grzhimailo, N. M. Kabachnik, and U. Becker, *J. Electron Spectrosc. Relat. Phenom.* **141**, 121 (2004).
  - [15] T. N. Rescigno, B. H. Lengsfeld, and A. E. Orel, *J. Chem. Phys.* **99**, 5097 (1993).
  - [16] S. Miyabe, C. W. McCurdy, A. E. Orel, and T. N. Rescigno, *Phys. Rev. A* **79**, 053401 (2009).
  - [17] J. C. Slater, *The Self-Consistent Field for Molecules and Solids: Quantum Theory of Molecules and Solids* (McGraw-Hill, New York, 1974), Vol. 4.